Peculiarities of focal conic structure formed near the cholesteric-isotropic phase transition

P. V. Dolganov,[1] K. D. Baklanova,[1,2] and V. K. Dolganov[1]
[1]*Institute of Solid State Physics, Russian Academy of Sciences, 142432, Chernogolovka, Moscow Region, Russia*
[2]*National Research University Higher School of Economics, 101000, Moscow, Russia*

(Received 24 May 2022; accepted 17 June 2022; published 13 July 2022)

Focal conic structure formed near the transition from the cholesteric liquid crystal phase into isotropic liquid is studied in planar cells with a combination of optical methods. Employing a procedure with slow variation of temperature, we manage to obtain regions of periodic focal conic structure with two-dimensional square ordering in the plane of the cell. Using ordered samples and materials with selective reflection in the visible spectral range, we obtain spectral and microscopic optical data which deepen our knowledge of the focal conic structure.

DOI: 10.1103/PhysRevE.106.014703

I. INTRODUCTION

Chiral liquid crystals form numerous structures with nontrivial ordering and fascinating optical properties [1,2]. The simplest example is the chiral nematic or cholesteric liquid crystal, which has a one-dimensional helical structure. More complex structures formed by chiral liquid crystals are blue phases [3–6], which appear at high chirality (short helical pitch) near the transition from cholesteric to isotropic phase [4,5]. Blue phases can be considered as three-dimensional ordered structures of defects. No less interesting structure is found at larger value of the helical pitch, namely, so-called focal conic domains [7]. Focal conic domains were first observed in smectic liquid crystals in the beginning of the 20th century [8,9]. Analysis of the focal conics structure led Friedel and Bragg to the fundamental conclusion that the smectic *A* phase has layered ordering [9,10]. In these structures the deformations of smectic layers are mainly related to their bending. The layer thickness in focal conic domains is constant, which is favorable energetically. Focal conics domains contain a pair of line singularities, in particular an ellipse and a hyperbola [1,11,12]. The singularities are conjugated, i.e., one of the focuses of the ellipse is the apex of the hyperbola and vice versa. Smectic layers are perpendicular to the straight line connecting points on the ellipse and on the hyperbola. The layers in the focal domains form Dupin cycles [1].

In cholesteric liquid crystals focal conic domains are also frequently observed [13–16]. Complex structures can be induced in cholesteric in confined geometry by imposing appropriate boundary conditions or by external action such as mechanical dilation [2,14,16–19]. Essential achievements in the studies of domain textures of cholesteric liquid crystals were made in the 1970s by Bouligand [20–22]. In particular, he described so-called polygonal texture and proposed a model of the organization of liquid crystal in this state [20]. Employing a liquid crystal with a large pitch (several microns) enabled him to see the regions near the surface with cholesteric helix oriented in the sample plane. Focusing the microscope objective near the upper and lower glass plates of the cell showed the existence of two systems of circular domains shifted with respect to each other at the two surfaces [20]. Similar textures were observed not only in thermotropic but also in lyotropic and lipid chiral liquid crystals [23–27]. In the last decade, progress in the experimental techniques led to better understanding of these defect structures [28–34]. Visualization of the cholesteric layers was performed with atomic force microscopy [14,28,29], scanning and transmission electron microscopy [28,29,34], and fluorescence confocal polarizing microscopy [35]. In optical transmission spectra, a shift of the photonic band was observed at the transition from the planar cholesteric to domain structure [28,31,33]. It is worth noting that similar structures are found in living organisms, in particular in the cuticle of certain types of beetles [31–33]. However, in spite of a long history of studies, the description of structure and optical properties of cholesteric focal conic domains are far from complete. In particular, experiments are often performed on irregular or disordered domains which may obscure some of their intrinsic properties.

In this paper we systematically investigated the focal conic structure formed near the cholesteric-isotropic transition in planar cells. We succeeded in obtaining a periodic two-dimensional ordered structure. Optical properties of the periodic focal conic structure have been studied in detail. To clarify the organization of the structure we performed observations of the same region at the top and at the bottom surfaces of the sample. This procedure was essential for determination of the structure. Complex dependence of the optical pattern of the sample on light polarization was observed. We measured spectra of single and double reflections of light and found their localization in different regions of the ordered structure. Our results enable us to establish correlation between photonic properties and structure of focal conics, which is in agreement with previously obtained data and with the parabolic focal conic model proposed by Rosenblatt *et al.* [36].

The organization of this paper is as follows. Section II describes chiral mixtures used in the investigations and lists

the experimental methods as well as the procedure employed to obtain the periodic focal conic structure. In Sec. III we describe in detail our optical and spectral studies. Section IV is devoted to discussion of the experimental observations and structure of focal conics. The main results of our investigations and further prospects are summarized in Sec. V, Conclusion and Perspectives.

II. EXPERIMENTAL DETAILS

Mixtures of wide temperature range nematic E7 with chiral material CB15 from Synthon Chemicals (Bitterfeld-Wolfen, Germany) were used for our investigations. Mixtures with weight content X of CB15 from 3.5% to 56% were employed. In our investigations we used two types of cells: planar optical cells with gaps from 9 to 20 μm (Instec Inc.), and homemade wedge cells. The liquid crystal material was capillary filled into the cell. The cells with the liquid crystal were placed in the Linkam LTS120 heating/cooling stage or Mettler Toledo FP82HT hot stage. For optical studies, an Olympus BX51 microscope was employed in transmission and reflection mode (50× objective, N.A. = 0.5). Images of the samples were recorded with a Baumer VCXU-02C video camera and Nikon D3300 camera. Reflection spectra in the visible and near-infrared range were measured with an Avantes-2048 fiber optic spectrometer coupled to the microscope.

At low temperature far from the transition to the isotropic phase all the investigated mixtures possess the cholesteric phase with planar texture (helical axis perpendicular to the plane of the cell). The cholesteric pitch p was determined using two methods. For chiral content $X < 35\%$ the pitch was measured using Grandjean-Cano wedge cells [2]; for $X \geqslant 27\%$ the pitch was found from selective reflection or transmission spectra. In the intermediate range of chiral additive content, the pitch was measured with both methods. The values determined by these measurements in the same mixture are close to each other. In E7/CB15 mixtures the helical pitch weakly depends on temperature. In a wide interval of concentrations the dependence of the wave number of the cholesteric helix $q = 2\pi/p$ on X is linear. The slope of the linear dependence gives the helical twisting power of CB15 in E7 about 7.2 μm^{-1}. This value is in good agreement with previously reported data [37]. The temperature of the transition into the isotropic phase decreases monotonically with increasing X.

To obtain the focal conic structure we slowly heated the sample in the cholesteric phase with planar texture (at a rate about 0.1 °/min). Near the temperature of the transition to the isotropic phase, regions with oblique orientation of the helix appear in the sample. If heating is stopped at an appropriate moment (in a temperature range about 1 °C before the transition to the isotropic phase), the planar texture transforms into the focal conic structure. In some regions a regular two-dimensional periodic pattern is formed. The reason for the appearance of the focal conic structure can be weakening of the surface anchoring near the cholesteric-isotropic transition. If the focal conic structure is kept at a constant temperature after preparation, it remains for a long time. On cooling the focal conic structure can be preserved at room temperature for months. Usually the appearance of the sample transforms

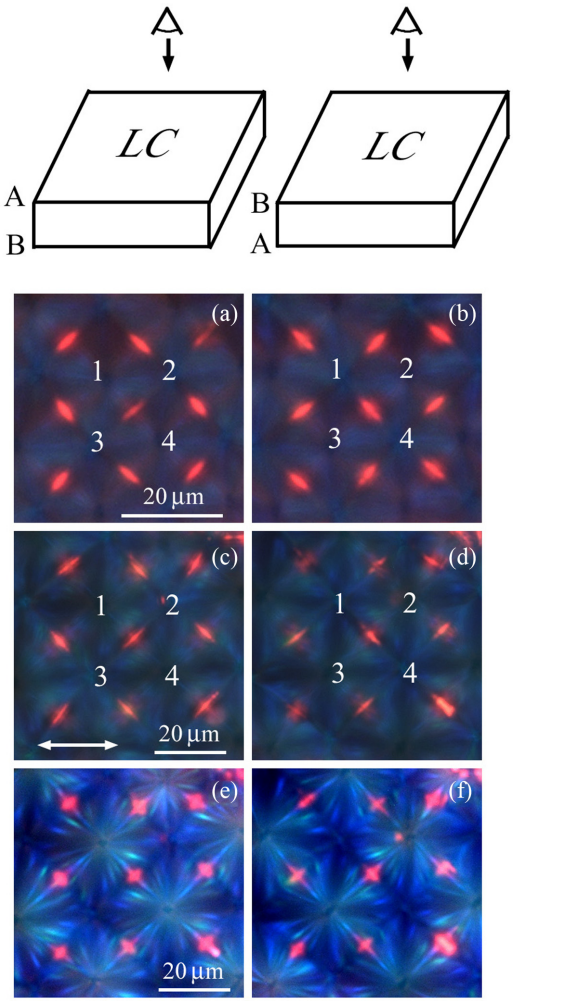

FIG. 1. Photographs of a two-dimensional periodic structure (focal conic domains) with square ordering. Reflection, crossed polarizers. Photographs (a) and (b) and (c)–(f) were taken on two different samples [notice that the length of the scale bars in (a) and (c) differs by 40%]. Focus near the surface of the cell (a)–(d), focus in the interior of the cell (e), (f). Photographs (e) and (f) are brighter with respect to (c) and (d) due to larger exposure. Photographs (a), (c), and (e) were taken from the top side of the sample (A); photographs (b), (d), and (f) were taken from the bottom side (B). The upper panels demonstrate the observation of the sample from the top side A (left) and from the bottom side B (right). Numbers 1–4 in (a)–(d) indicate domains forming the periodic structure. Thickness of the samples $h = 20\,\mu$m. The double-headed arrow in (c) shows the rubbing direction. CB15 contents in the mixture $X = 35\%$.

slightly, but the main features of the structure can remain the same as at high temperature. We observed formation of the periodic focal conic domain structure near the cholesteric-isotropic transition in mixtures with values of the helical pitch in the range 325 nm $\lesssim p \lesssim$ 900 nm. In the following sections we mainly illustrate our findings with results on cholesteric with pitch about 400 nm.

III. RESULTS

Figure 1 shows an example of the two-dimensional structure observed in reflected light with crossed polarizers. The

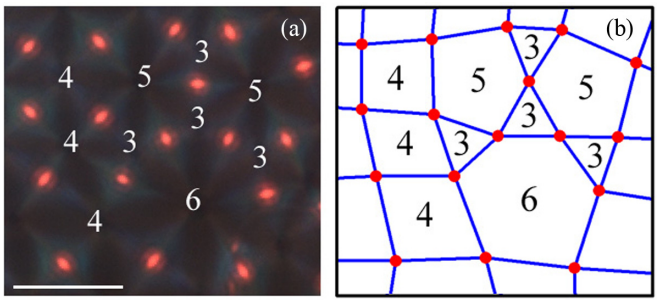

FIG. 2. Photograph of a region of the focal conic structure composed of different types of polygons (a). Partition of the structure into polygons is shown in (b). The number of vertices in the polygons is indicated in polygon centers. Besides tetragons (squares in the ideal structure) the structure contains triangles, pentagons, and a hexagon. Reflection, crossed polarizers. The scale bar in (a) is 20 μm.

polarizers are oriented along the horizontal and vertical directions. The appearance of the structure depends on the position of the microscope focus. In particular, Figs. 1(a) and 1(c) show photographs taken when the focus is near the upper surface of the cell. A nearly square ordering is observed. The structure is composed of a regular array of red domains on darker blue background. The periodicity of the structure can somewhat vary from sample to sample. For illustration, in Figs. 1(a) and 1(c) we show photographs of two samples with the same thickness and cholesteric pitch: the pattern of the red domains is the same, but the period differs by about 40%. In Fig. 1(c) the distance between neighboring red domains is close to the cell thickness. The red domains look elongated with the long axis under $\pm 45^\circ$ with respect to the horizontal direction. The transverse size of the red domains is about 1.5–2 μm; the length is several times larger. Neighboring red domains have alternating orientation (i.e., $\pm 45^\circ$ and -45°). For clarity of further description, we denote the regions of the sample surrounded by four red domains by numbers 1–4. The periodic structure can be regarded as formed by these square domains.

Besides the structure with nearly square ordering (Fig. 1), the red domains can form other types of polygons. Such polygons can be observed in particular near the boundary of regions with square ordered structure. A photograph of an intermediate region between ordered and disordered areas is given in Fig. 2(a). For clarity, we show partition of the structure into polygons in Fig. 2(b). The number of vertices in each polygon is indicated in the figure. In the left part of the photograph the structure is composed of tetragons, which correspond to squares in the perfect structure. In the right part of the photograph the structure is distorted. Different types of polygons appear: triangles, pentagons, and a hexagon. Let us note that the disordered structure of polygons retains certain regularity. In particular, in the vertices of each polygon (Fig. 2) the orientation of the red domains is uniform, that is, either all the long axes of red domains are directed towards the center of the polygon or all the long axes are oriented perpendicular to the direction towards the polygon center. In nearest domains the orientation of the long axes is opposite (towards the polygon center in one domain and in the perpendicular direction in the other domain).

To investigate in detail the periodic structure, we observed the same region of the sample not only from the top side A (left column of Fig. 1), but also from the bottom side B (right column of Fig. 1). For observations from the bottom side the sample was turned upside down, so that surfaces A and B change places. This procedure also flips the view of the sample in the focal plane of the microscope. To match the regions in the photograph with the photograph taken from the top side, we flipped the recorded image in the vertical direction. As a result, the orientation of the sample in the two photographs coincided [see the illustrations, letters LC in the upper panels in Fig. 1, and the red defect in the top right corner of Figs. 1(c)–1(f)]. Photographs of the samples from the top side A and from the bottom side B are given correspondingly in the left and right columns in Fig. 1. In particular, Fig. 1(b) shows a photograph taken on the same region as in Fig. 1(a) when the focus is near the surface B of the cell. When the sample is viewed from two opposite sides, the orientation of the red domains changes by 90° [compare Figs. 1(a) and 1(b)]. In Fig. 1(a) in domains 1 and 4 the orientation of the red elongated domains is circular. In domains 2 and 3 the orientation of the red domains is radial. When the same region is viewed from the bottom [Fig. 1(b)], in domains 1 and 4 the red domains are oriented in radial directions, and in domains 2 and 3 the red domains have circular orientation. Analogous alternation of the orientation of elongated red domains is observed when the sample of Fig. 1(c) is viewed from the bottom side B [Fig. 1(d)]. We may guess that two systems of domains with opposite orientation exist in the structure near the top and the bottom.

The darker blue background also possesses a number of specific features. We found that red and blue domains are in focus at different height. Photographs of the same region as in Figs. 1(c) and 1(d) with the focus in the interior of the sample are shown in Figs. 1(e) and 1(f). With such position of the focus the red domains look nearly similar to each other. The appearance of the blue background is modified. Blue starlike patterns become visible. In Fig. 1(e) the centers of the stars are located in the centers of domains 1 and 4. When viewed from the top and from the bottom of the sample, the blue pattern is shifted [Figs. 1(e) and 1(f)]. In particular, the centers of the stars in Fig. 1(f) are located in the centers of domains 2 and 3.

Figure 3 shows the same region as in Figs. 1(c)–1(f) viewed in transmission with crossed polarizers [Fig. 3(a)] and with one horizontal polarizer [Fig. 3(b)]. Focus is in the interior of the cell [Fig. 3(a)] and near the upper surface of the cell [Fig. 3(b)]. The pattern in transmission, as well as in reflection, changes with the change of the microscope focus and also changes with the orientation of the polarizers. However, analysis of the pattern in transmission is more complicated than in reflection, so we will mainly rely on the results observed in reflected light.

In samples with larger cholesteric pitch, colors of the periodic structure in reflection are redshifted. Figure 4 shows an example of the periodic structure formed in a sample with cholesteric pitch $p \approx 530$ nm, where the cholesteric photonic band is at about 860 nm. In reflected light image [Fig. 4(a)] a periodic starlike pattern is visible. This pattern resembles

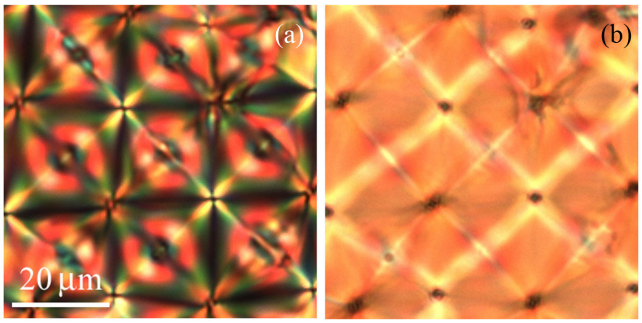

FIG. 3. Photographs of the focal conic domains in transmission, the same region as in Figs. 1(c)–1(f). Polarizers are crossed (a), single horizontal polarizer (b). Focus is in the interior of the cell (a); focus is close to the upper surface of the sample (b).

the background pattern in Fig. 1, but its color is red, whereas the starlike pattern in Fig. 1 is blue. Elongated domains (analogues of red domains in Fig. 1) are not visible. This is understandable since their color is expected to be in the near-infrared spectral range. The pattern in transmission [Fig. 4(b)] shows square ordering, as in the mixture with shorter helical pitch [Fig. 3(a)].

To gain more insight in the nature of the periodic structure, we investigated its spectral properties. Reflection spectra measured in right and left circularly polarized light, as usually done for chiral photonic crystals, are shown in Fig. 5. The solid green curve and the dashed black curve [Fig. 5(a)] show spectra measured on the planar texture of the cholesteric phase with pitch $p \approx 400$ nm. Red and blue curves [Fig. 5(b)] are the spectra measured on the focal conic structure in the same mixture. In the cholesteric planar texture [Fig. 5(a)] the selective reflection band is pronounced only in right circular (intrinsic) polarization. In the focal conic texture [Fig. 5(b)] the spectrum possesses a peak at the wavelength close to selective reflection of cholesteric and a broad band at shorter wavelength. The circular dichroism in the focal conic texture is substantially smaller than in planar cholesteric. The long-wavelength band has somewhat larger intensity in right circular polarization (red solid curve) than in left circular polarization (blue dashed curve), but in both polarizations the band is relatively strong.

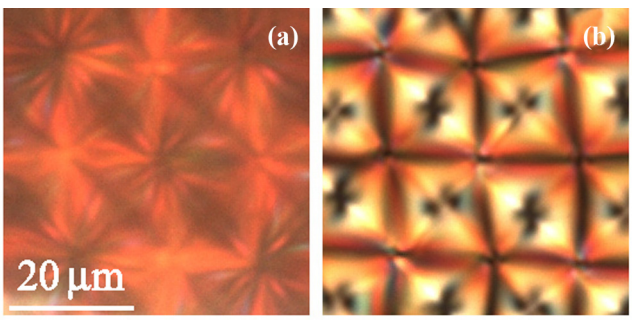

FIG. 4. Focal conic structure in the mixture with cholesteric pitch about 530 nm ($X = 26.5\%$). The photographs were taken in reflection (a) and in transmission (b) with crossed polarizers. $h = 20\,\mu$m. Focus is in the interior of the cell.

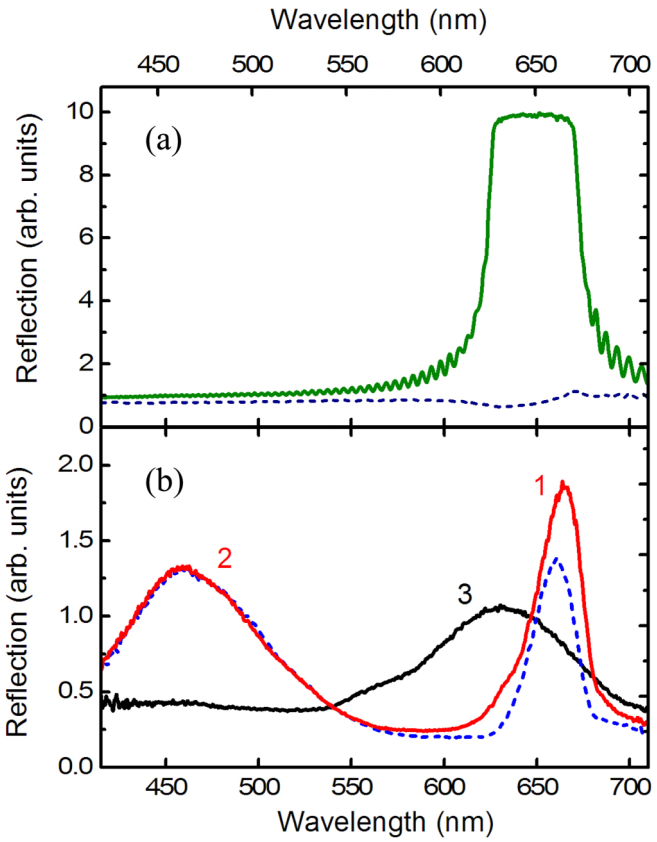

FIG. 5. Reflection spectra of planar cholesteric with pitch about 400 nm (a) and focal conic structure (b). Solid curves show spectra measured in light of right circular polarization; dashed curves give spectra measured in left circular polarization. Two peaks (1) and (2) in the spectra of the focal conic structure can be attributed to red and blue regions in the photograph [Fig. 1(a)]. $X = 35\%$. The curve (3) in (b) shows the reflection spectrum of the focal conic texture in the mixture with larger cholesteric pitch about 530 nm ($X = 26.5\%$).

As to the short-wavelength band, its intensity is close in both circular polarizations.

IV. DISCUSSION

Let us now discuss in detail the obtained experimental data and organization of cholesteric in the periodic structure. We will focus on the periodic structure with red elongated domains (Fig. 1), since its analysis is most straightforward. To start, observation of the sample from the top and bottom sides (left and right columns of Fig. 1) unambiguously indicates that in our focal conic structure there exist two systems of domains shifted with respect to each other. Figure 6(a) schematically shows the positions of red domains (Fig. 1) near the top surface. Previously systems of circular spirals or concentric circles were observed on the surface of cholesteric samples [14,16,20,25,28]. Their appearance is due to the exit of cholesteric "layers." In the place of contact of two spirals or circles the orientation of cholesteric "layers" differs from orientation within spirals or circles [20,25]. In our case, circles drawn in Fig. 6(a) contact at the location of the elongated red domains. Different colors in reflection are an indication of different orientation of the cholesteric axis, as discussed

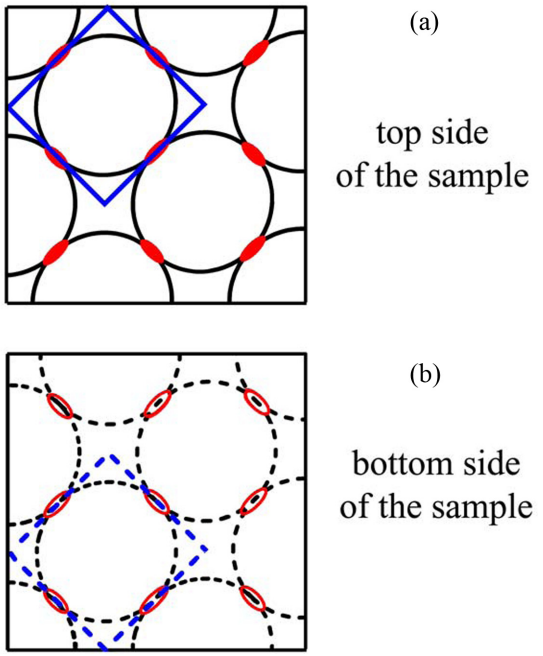

FIG. 6. Schematic representation of the periodic structure at the top (a) and bottom (b) surfaces of the sample. The structure is composed of a periodic system of domains (represented by solid and dotted circles). In the place of contact of the neighboring circles, elongated regions correspond to domains which are red in reflection. The square cell at the surface of the sample is indicated by blue lines [solid in (a), dotted in (b)].

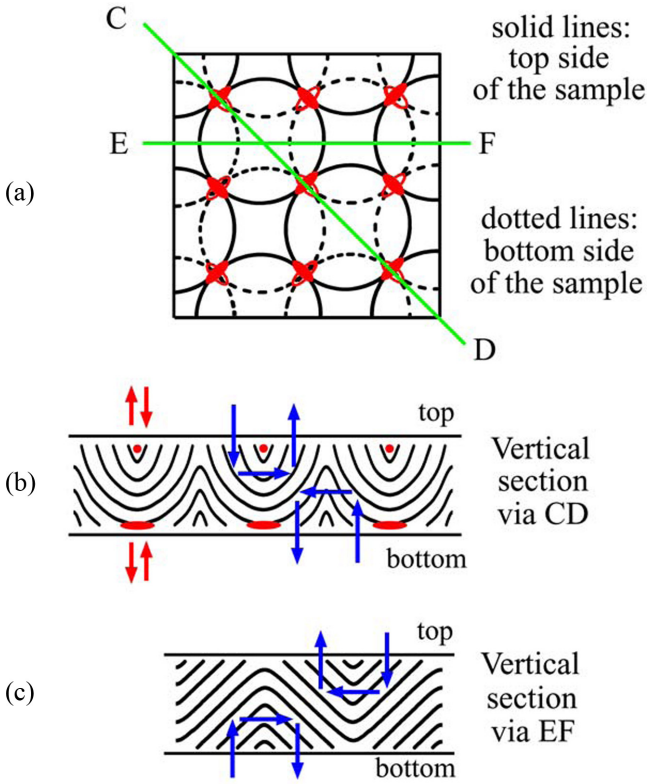

FIG. 7. (a) Schematic representation of the periodic structure with superimposed top and bottom surfaces of the sample (Fig. 6). The red elongated regions at the top and bottom surfaces of the sample are perpendicular to each other. Sections of the structure perpendicular to the plane of the cell along directions CD and EF are shown in (b) and (c). Reflections from different regions of the structure are shown by arrows. Backward reflection results in the peak centered at $\lambda_1 \sim 660$ nm (red arrows). Double reflections from two sets of cholesteric "layers" oriented approximately under $\pm 45^\circ$ with respect to sample normal give rise to a band at $\lambda_2 \sim 460$ nm (blue arrows).

further. The cell of the square structure near the upper surface [domain 1 in Fig. 1(a)] is shown by blue lines. Near the bottom surface [Fig. 6(b)] the similar unit cell is shifted with respect to the upper surface.

Figure 7(a) shows the systems of domains in the top and bottom parts of the sample superimposed on each other. The elongated red domains in the top and bottom parts are perpendicular to each other in accordance with the observations (Fig. 1). Three-dimensional representation of the unit of the periodic structure is shown in Fig. 8. The square in the top of the sample corresponds to the square drawn in Fig. 6(a). The vertical dotted lines connect the elongated red domains near the top and bottom of the sample.

Colors of reflected light images (Figs. 1 and 4) and the bands in reflection spectrum [Fig. 5(b)] could be explained using the representation of the periodic structure (Figs. 7 and 8) and on the basis of selective reflections of planar cholesteric. Uniformly oriented cholesteric with the helical axis perpendicular to the cell plane is characterized by a single selective reflection band centered at $\lambda_{Ch} = pn$, where n is the average refractive index perpendicular to the helical axis [2]. According to the assumption of Bouligand for the cholesteric polygonal structure [20], in the places where circular spirals touch each other, the helical axis is oriented perpendicular to the sample plane. Our data confirm this assumption. In reflection these regions show the same characteristic color (selective reflection wavelength) as the planar cholesteric. To the best of our knowledge such reflection has not been observed in the focal conic structure. We observed such localized reflection in the centers of the edges of the squares in the upper and lower parts of the sample. Figure 7(b) shows the vertical section of the focal conic structure along direction CD [Fig. 7(a)]. This section passes through red domains in the top and bottom parts of the sample. The distance between red domains along this section is in $\sqrt{2}$ times larger than between neighboring red domains in the structure [Fig. 7(a)]. While the wavelength of reflection from red domains corresponds to planar cholesteric (Fig. 5), the intensity of this reflection is substantially lower since the size of such regions is much smaller (Fig. 1). The band width in cholesteric is large and is mainly determined by the width of the photonic zone [2]. In the focal conic structure the band is narrower [Fig. 5(b)]. At present, to the best of our knowledge, there is no theory describing the spectral properties of the focal conic texture.

A structure with spatially varying orientation of the cholesteric helix can give rise to multiple reflections. Appearance of additional reflection in the focal conic structure is illustrated in the drawings of sections along directions CD and EF [Figs. 7(b) and 7(c)]. Oblique orientation of the cholesteric helix leads to a shift of the reflection to shorter wavelengths

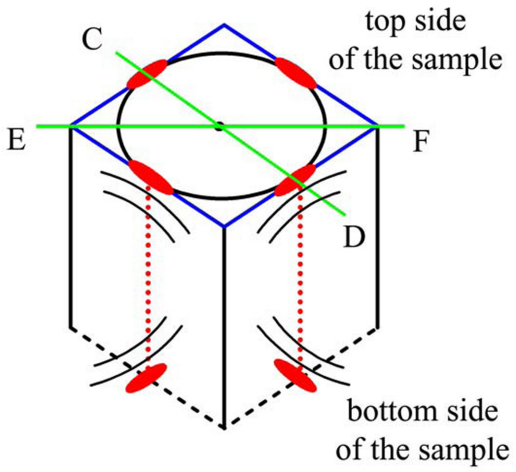

FIG. 8. Schematic three-dimensional representation of the cell of the periodic structure. The upper square corresponds to the cell indicated in Fig. 6(a). The orientation of cholesteric "layers" is schematically shown in the middle of the edges of the unit square near the top side and the bottom side. In these regions the helical axis is perpendicular to the plane of the sample. Sections along lines CD and EF are shown in Fig. 7. Vertical dotted lines connect the red domains near the upper and lower surfaces of the sample.

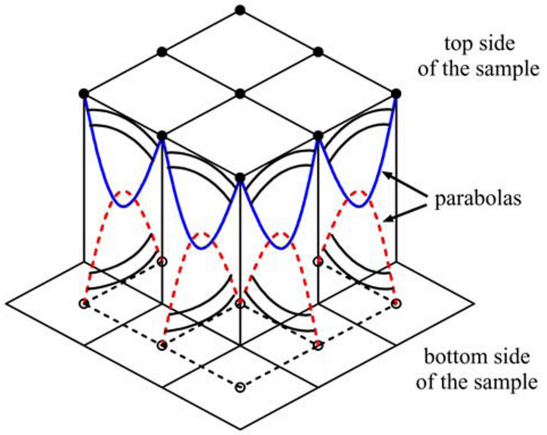

FIG. 9. Parabolic focal conic domain structure (after Rosenblatt *et al.* [36]). Solid and open dots show square ordering at the top and the bottom side of the sample. The planes of two parabolic line defects (solid blue and dashed red curves) are perpendicular to each other. Solid curves near the top and the bottom of the sample show cholesteric "layers."

$\lambda = pn\cos\alpha$, where α is the tilt angle of the helix. Reflected light propagates under angle 2α with respect to the normal to the sample plane. If $\alpha = 45^\circ$, the reflection occurs under 90°, and two consecutive reflections would result in the backward reflection of light. Such backward reflection was observed in our experiment. Red and blue arrows in Figs. 7(b) and 7(c) show backward reflection from cholesteric with the helical axis perpendicular to the sample plane [λ_1, band 1 in Fig. 5(b)] and double reflections from cholesteric oriented obliquely under about 45° [λ_2, band 2 in Fig. 5(b)]. Assuming a constant periodicity of the cholesteric structure, the short-wavelength peak should be observed at $\lambda_2 = \lambda_1/\sqrt{2}$, which is close to the experimentally found value (Fig. 5). The section of the structure along the direction EF does not pass through red domains (Figs. 7 and 8). From regions along the line EF, only double blue reflections can be observed.

Double backward reflections can be observed from two planar structures with orientation under ±45° or in more complex geometry from a two-dimensional hexagonal lattice of cholesteric droplets with radial orientation of the helix [30,32]. If backward selective reflection from cholesteric is in the red spectral range, a bright blue starlike pattern is observed, similar to our case, due to double reflections. However, our reflection pattern from the focal conic domains is essentially more complex than in the structure of cholesteric droplets [30,32]. In particular, the structure and spatial localization of reflections from the droplets is the same if viewed from the two sides of the sample. In our case, the reflection pattern and the structure near the bottom surface are shifted with respect to the other surface.

We remind that adjusting the focus of the microscope shows that the elongated red domains (Fig. 1) are located closer to the upper plate of the cell, and the blue-colored starlike pattern is in focus at a lower level. This is in agreement with the structure shown in Figs. 7 and 8. Another argument in support of this structure is found in the cholesteric with larger pitch (mixture with $X = 26.5\%$ where the selective reflection band in the cholesteric phase is centered at $\lambda_1 \approx 860$ nm). The reflection spectrum of the focal conic texture has a wide band centered at λ_2 about 620 nm [Fig. 5(b), band 3]. This corresponds to the ratio of wavelengths $\lambda_1/\lambda_2 \approx 1.4$. These observations confirm the assumption that the two bands (1 and 2) are related to reflections from regions with the helix perpendicular to the surface and from regions where the helix is tilted by 45° with respect to the surface (Fig. 7). To the best of our knowledge, such spectral investigations on a periodic confocal structure have not been performed to date. For a quantitative description and understanding the spectral properties of the square texture, the polarization characteristics of reflected and transmitted light, detailed numerical calculations might be necessary. This would be the subject of future work.

The square texture observed in our experiment is similar to the structure of parabolic focal conic domains discovered by Rosenblatt *et al.* in smectic *A* liquid crystal [36]. In their study the two-dimensional defect pattern was induced by dilation [36]. To explain the observed features the authors [36] proposed that bending of smectic layers could lead not only to existence of conjugated ellipse and hyperbola defects, but also to two conjugated parabolas (Fig. 9): the apex of one parabola is the focus of the other parabola and vice versa. The planes of the two parabolas are perpendicular to each other. The main features of the texture obtained in our experiment are consistent with the parabolic focal conic structure. For example, in parabolic focal conics the textures at the bottom and at the top of the sample are shifted with respect to each other by half of the square diagonal (Fig. 9). The same shift at the bottom with respect to the top follows from our data (Figs. 6 and 7). We anticipate that further investigation of the focal conics in different materials will elucidate the necessary conditions for appearance of the periodic structures.

A question about the stability of the periodic focal conic structure may arise. In our experiments, the focal conic domains were obtained on heating close to the cholesteric-isotropic transition, similar to blue phases, which form at shorter helical pitch. Blue phases can be overcooled to low temperatures and exist at low temperature as a metastable state. Spontaneous formation of the periodic focal conic structure on heating and its preservation on cooling allows us to guess that this structure in our samples is a stable state in confined geometry near the cholesteric-isotropic transition and a metastable state far from the transition, analogous to the blue phases.

V. CONCLUSION AND PERSPECTIVES

In this paper we in detail investigated focal conic structure with square ordering formed in cholesteric liquid crystals with submicrometer cholesteric pitch. This structure appears spontaneously near the transition into the isotropic phase. Observations of the same regions from the top and from the bottom side of the sample enabled us to elucidate the ordering in the structure. Spectral properties of the periodic structure were studied. Two bands were observed in reflection spectra, and their origin has been explained. A model of the organization of cholesteric layers in the periodic structure is described and discussed. We hope our work advances the understanding of the cholesteric focal conic domain structure.

However, many questions remain open. Creation of a theory describing periodic focal conic structures, comparing their energy with the energy of uniform cholestreric (as done earlier for the blue phases), is a topical problem for future research. Chirality in cholesteric creates cholesteric "layers" that bend and form focal conic structures (similar to smectic focal conics). It is not clear whether chirality is essential only for creating "layers" or whether it also contributes to bending of the helical axis and formation of focal conics.

ACKNOWLEDGMENTS

The reported study was supported by the State Assignment of ISSP RAS. The authors report no competing interests.

[1] M. Kleman and O. D. Lavrentovich, *Soft Matter Physics: An Introduction* (Springer, New York, 2003).

[2] P. Oswald and P. Pieranski, *Nematic and Cholesteric Liquid Crystals: Concepts and Physical Properties Illustrated by Experiments* (Taylor and Francis, Boca Raton, FL, 2005).

[3] S. Meiboom and M. Sammon, Blue phases of cholesteryl nonanoate, Phys. Rev. A **24**, 468 (1981).

[4] V. A. Belyakov and V. E. Dmitrienko, The blue phase of liquid crystals, Sov. Phys. Usp. **28**, 535 (1985).

[5] D. C. Wright and N. D. Mermin, Crystalline liquids: The blue phases, Rev. Mod. Phys. **61**, 385 (1989).

[6] H. Kikuchi, Liquid crystalline blue phases, in *Liquid Crystalline Functional Assemblies and Their Supramolecular Structures*, edited by T. Kato, *Structure and Bonding* (Springer, Berlin, 2017), Vol. 128, pp. 99–117.

[7] I. Dierking, *Textures of Liquid Crystals* (Wiley-VCH, Weinheim, 2003).

[8] G. Friedel and F. Grandjean, Observations géométriques sur les liquides à coniques focales, Bull. Soc. Fr. Miner. Cristallogr. **33**, 409 (1910).

[9] G. Friedel, Les états mésomorphes de la matière, Ann. Phys. **9**, 273 (1922).

[10] W. Bragg, Focal conic structures, Trans. Faraday Soc. **29**, 1056 (1933).

[11] Y. Bouligand, Recherches sur les textures des états mésomorphes—1. Les arrangements focaux dans les smectiques: Rappels et considérations théoriques, J. Phys. **33**, 525 (1972).

[12] O. D. Lavrentovich, Hierarchy of defect structures in space filling by the flexible smectic-A layers, Sov. Phys. JETP **64**, 984 (1986).

[13] G. W. Gray, The mesomorphic behaviour of the fatty esters of cholesterol, J. Chem. Soc. 3733 (1956).

[14] R. Meister, M.-A. Hallé, H. Dumoulin, and P. Pieranski, Structure of the cholesteric focal conic domains at the free surface, Phys. Rev. E **54**, 3771 (1996).

[15] W-R. Chen and J. C. Hwang, The phase behaviour and optical properties of a nematic/chiral dopant liquid crystalline mixture system, Liq. Cryst. **31**, 1539 (2004).

[16] L. Tran, M. O. Lavrentovich, G. Durey, A. Darmon, M. F. Haase, N. Li, D. Lee, K. J. Stebe, R. D. Kamien, and T. Lorez-Leon, Change in Stripes for Cholesteric Shells via Anchoring in Moderation, Phys. Rev. X **7**, 041029 (2017).

[17] N. A. Clark and P. S. Pershan, Light Scattering by Deformation of the Plane Texture of Smectic and Cholesteric Liquid Crystals, Phys. Rev. Lett. **30**, 3 (1973).

[18] N. A. Clark and R. B. Meyer, Strain-induced instability of monodomain smectic A and cholesteric liquid crystals, Appl. Phys. Lett. **22**, 493 (1973).

[19] T. Yu, L. Luo, B. Feng, and X. Shang, Anchoring effect on the stability of a cholesteric liquid crystal's focal conic structure, Chinese J. Phys. **50**, 804 (2012).

[20] Y. Bouligand, Recherche sur les textures des etats mesomorphes. 2. Les champs poligonaux dans les cholesteriques, J. Phys. **33**, 715 (1972).

[21] Y. Bouligand, Recherches sur les textures des états mésomorphes. 3. Les plages à éventails dans les cholestériques, J. Phys. **34**, 603 (1973).

[22] Y. Bouligand, Defects and textures in cholesteric analogues given by some biological systems, J. Phys. **36**, C1-331 (1975).

[23] A. M. Donald, C. Viney, and A. P. Ritter, The parabolic focal conic texture in a lyotropic liquid-crystalline polymer, Liq. Cryst. **1**, 287 (1986).

[24] S. Guido, Cholesteric textures of aqueous hydroxypropylcellulose solutions, Mol. Cryst. Liq. Cryst. **266**, 111 (1995).

[25] M. Yada, J. Yamamoto, and H. Yokoyama, Spontaneous formation of regular defect array in water-in-cholesteric liquid crystal emulsions, Langmuir **18**, 7438 (2002).

[26] M. Yada, J. Yamamoto, and H. Yokoyama, Regular defect array formed after shear in water-in-cholesteric liquid crystal emulsions, Mol. Cryst. Liq. Cryst. **409**, 119 (2004).

[27] S. A. Asher and P. S. Pershan, Parabolic focal conics and polygonal textures in lipid liquid crystals, J. Phys. **40**, 161 (1979).

[28] G. Agez, R. Bitar, and M. Mitov, Color selectivity lent to a cholesteric liquid crystal by monitoring interface-induced deformations, Soft Matter **7**, 2841 (2011).

[29] A. Bobrovsky, O. Sinitsyna, S. Abramchuk, I. Yaminsky, and V. Shibaev, Atomic force microscopy study of surface topography of films of cholesteric oligomer- and polymer-based mixtures with photovariable helix pitch, Phys. Rev. E **87**, 012503 (2013).

[30] J. Fan, Y. Li, H. K. Bisoyi, R. S. Zola, D. Yang, T. J. Bunning, D. A. Weitz, and Quan Li, Light-directing omnidirectional circularly polarized reflection from liquid-crystal droplets, Angew. Chem. Int. Ed. **54**, 2160 (2015).

[31] G. Agez, C. Bayon, and M. Mitov, Cholesteric microlenses and micromirrors in the beetle cuticle and in synthetic oligomer films: A comparative study, Proc. SPIE **10125**, 10125OU (2017).

[32] H. K. Bisoyi, T. J. Bunning, and Quan Li, Stimuli-Driven control of the helical axis of self-organized soft helical superstructures, Adv. Mater. **30**, 1706512 (2018).

[33] A. Jullien, A. Scarangella, U. Bortolozzo, S. Residori, and M. Mitov, Nanoscale hyperspectral imaging of tilted cholesteric liquid crystal structures, Soft Matter **15**, 3256 (2019).

[34] T. Orlova, R. Plamont, A. Depauw, and N. Katsonis, Dynamic spirals of nanoparticles in light-responsive polygonal fields, Small **15**, 1902419 (2019).

[35] B. I. Senyuk, I. I. Smalyukh, and O. D. Lavrentovich, Undulations of lamellar liquid crystals in cells with finite surface anchoring near and well above the threshold, Phys. Rev. E **74**, 011712 (2006).

[36] Ch. S. Rosenblatt, R. Pindak, N. A. Clark, and R. B. Meyer, The parabolic focal conic: A new smectic A defect, J. Phys. **38**, 1105 (1977).

[37] S.-W. Ko, S.-H. Huang, A. Y.-G. Fuh, and T.-S. Lin, Measurement of helical twisting power based on axially symmetrical photo-aligned dye-doped liquid crystal film, Opt. Express **17**, 15926 (2009).